JOURNAL OF Applied Polymer SCIENCE

Influence of Inorganic Fillers on the Structural and Transport Properties of Mixed Matrix Membranes

Aik Chong Lua, Yi Shen
School of Mechanical and Aerospace Engineering, Nanyang Technological University, Singapore 639798, Republic of Singapore
Correspondence to: A. C. Lua (E-mail: address:maclua@ntu.edu.sg)

ABSTRACT: In this study, three types of inorganic fillers—fumed nano-SiO_2, synthesized mesoporous MCM-41, and zeolite 4A—were incorporated into P84 matrix to prepare mixed matrix membranes. The structural characteristics and transport properties of the resulting composite membranes were investigated. Scanning electron microscopy (SEM) and transmission electron microscopy (TEM) were used to observe the dispersion of the filler particles in the composite membranes. TEM micrographs verified that there were no nonselective pores at the particle–polymer interfaces of the composite membranes. Differential scanning calorimetry tests were conducted to investigate the structure of the composite membranes. The glass transition temperatures (T_g) of the P84/MCM-41 and P84/4A composite membranes were 11 and 30°C, respectively, above that of pure P84 membrane. But, the T_g value for the P84/SiO_2 composite membrane decreased by 22°C when compared with that of the P84 membrane. The density of the composite membrane was also measured to calculate its fractional free volume. Gas permeation tests showed that, among the three synthesized composite membranes, the P84/SiO_2 membrane had the best performance in terms of gas separation. P84/SiO_2 membrane exhibited 20, 63, 59, and 45% increases in the permeabilities of He, O_2, N_2, and CO_2, respectively, above those for the P84 membrane whilst maintaining comparable good selectivities. © 2012 Wiley Periodicals, Inc. J. Appl. Polym. Sci. 128: 4058–4066, 2013

KEYWORDS: copolymers; gas permeation; membranes; polyimides; selectivity

Received 24 May 2011; accepted 19 September 2012; published online 17 October 2012
DOI: 10.1002/app.38614

INTRODUCTION

Gas separation based on polymeric membranes has been of great interest in the separation of some industrially important gases due to their lower energy consumption and capital investments when compared with some traditional separation technologies.[1–3] However, polymeric membranes have been shown to suffer the trade-off relationship between permeability and selectivity,[4] which limits the applications of polymeric membranes for gas separation. Organic–inorganic composite membranes with the combination of the desirable attributes of polymeric matrix and inorganic fillers seemingly offer a very promising solution to improve the gas separation performance. Zeolites with similar pore sizes to the kinetic diameters of some gas molecules have been preferentially investigated to prepare mixed matrix membranes to use their molecular sieving ability.[5–8] For example, with careful preparations, Mahajan and Koros[7] obtained zeolite 4A-poly(vinyl acetate) mixed matrix membranes, which were free of defects and showed increased selectivity and slightly decreased permeability when compared with the poly(vinyl acetate) membranes. Wang et al.[8] prepared mixed matrix membranes by incorporating zeolite A nanocrystals into polysulfone (PSF), and the synthesized composite membranes showed better O_2 selectivity and permeability than the PSF membranes. Merkel et al.[9,10] reported that the incorporation of nanoscale nonporous particles (fumed SiO_2) into glassy polymers could dramatically enhance the permeability of the polymers as well as maintain their excellent selectivity. They suggested that these nanoparticles could change the polymer chain structures and increase the free volume of the polymer chains, which was favorable to the transport of gas molecules. Similarly, mesoporous materials MCM-41 and MCM-48 had also been incorporated into PSF to enhance the gas transport properties of the resulting membranes.[11,12] It was reported that the permeability of the mesoporous silica and PSF composite membranes increased proportionally with the weight percentage of mesoporous materials present in the composite membranes, and the selectivity remained almost constant as that of the pure PSF membranes.

Until now, for organic–inorganic composite membranes, many studies had focused on the choice of polymer matrix and inorganic fillers,[13–16] preparation methods,[17–19] and the control of properties of polymer–particle interface.[20–22] However, few

studies[23–25] had reported on the influence of the properties of the filler particles on the structure of polymer chains and the gas transport properties. In this study, three types of filler particles—fumed nano-SiO_2, synthesized MCM-41, and zeolite 4A, with different particle sizes, pore surface areas, and pore structures—were incorporated into the P84 matrix to prepare mixed matrix membranes. The structure properties and gas transport properties of the resulting composite membranes were investigated and systematically compared.

EXPERIMENTAL

Materials

Commercially purchased nanosilica and zeolite 4A powders were activated overnight at 180°C before use. P84 copolyimide (BTDA-TDI/MDI, copolyimide of 3,3′,4,4′-benzophenone tetracarboxylic dianhydride, and 80% methylphenylene-diamine + 20% methylene diamine) was supplied by HP Polymer GmbH, Austria. The solvent for the P84 copolyimide, *N*-methyl-2-pyrrolidinone (NMP), was purchased from Sigma Aldrich, Singapore. All these chemicals were used as received. Milli-Q ultrapure water was prepared in house. Materials for the MCM-41 preparation, including tetraethyl orthosilicate (TEOS), ammonia, and cetyltrimethylammonium bromide (C_{16}TAB), were obtained from Sigma Aldrich, Singapore and used as received.

Synthesis of MCM-41 Silica

Mesoporous MCM-41 silica was synthesized as follows[26]: typically, 11 g (0.03 mol) of C_{16}TAB was dissolved in distilled water, aqueous ammonia, and ethanol solution by stirring for 15 min. About 21 g (0.1 mol) of TEOS was then added to the solution. A solution with a molar composition of 1 TEOS : 0.3 C_{16}TAB : 13 NH_3 : 60 ethanol : 142 H_2O was obtained. After stirring for 30 min, the solution was transferred into a Teflon-lined autoclave and aged at 100°C for 24 h.The resulting solid was collected by filtration and washed with distilled water. The dried precursor powder was calcined at 550°C for 10 h to remove the template, and MCM-41 was produced.

Fabrication of Pristine P84 Dense Membranes

P84 powder was degassed overnight at 373°C under vacuum to remove any moisture present. Four grams of P84 was then dissolved in 20 g of NMP, and the mixture was stirred for 48 h at room temperature. After the removal of gas bubbles, the solution was cast onto glass substrates and dried at 110°C in an oven for 12 h. Once it was dry, the membrane was clamped between two Teflon plates in a vacuum oven, and the temperature was raised to 180°C and dwelled for 24 h.

Fabrication of Composite Membranes

The composite membranes were prepared using a similar method reported by Qiao et al.[27] The detailed procedures are as follows: a predetermined amount of inorganic fillers was added to the NMP solvent, and the mixture was ultrasonicated for 30 min. At first, 4% of the total amount of P84 was added into the solution. After the initial-loaded polymer was totally dissolved by stirring for 12 h and followed by a period of 30-min ultrasonication, the remaining P84 polymer was then added to the solution, and the mixture was stirred for a week at room temperature. Before casting, the mixture was sonicated for 30 min to remove any gas bubbles. The drying and heat treatments were identical to those for the pristine dense membrane. Three inorganic fillers—nonporous nanosilica, MCM-41, and zeolite 4 A—were used to prepare the composite membranes, and these were designated as P84/SiO_2, P84/MCM-41, and P84/4A, respectively. Four different weight percentages of inorganic fillers, that is, 4, 8, 12, and 15%, were used to prepare the composite membranes. However, the composite membranes with 12 and 15% inorganic fillers, especially for the 12 and 15% zeolite 4A, were brittle and cracked easily, resulting in erroneous permeability values. Consequently, the weight percentage of the inorganic filler was kept at 8% for all the composite membranes.

Characterization Methods

X-ray diffraction (XRD) patterns were obtained by a diffractometer (PW1820, Philip) equipped with Cu Kα X-ray radiation. The N_2 adsorption–desorption isotherms were obtained using the accelerated and surface area porosimetry system (ASAP 2010, Micromeritics). Before the test, the sample was out-gassed overnight at 200°C in a vacuum oven. The pore surface area was calculated using the Brunauer–Emmett–Teller (BET) method; the pore volume and pore size were calculated by the Barret–Joyner–Halenda (BJH) method.

A scanning electron microscope (JSM-5600LV, JEOL) was used to examine the morphology of the membrane and the dispersion of the inorganic fillers on the composite membranes. Before testing, all the scanning electron microscopy (SEM) samples were coated with platinum. For the cross-sectional views, the samples were prepared by fracturing the membranes in liquid nitrogen.

A transmission electron microscope (TEM; JSM2010, JEOL) was used to study the dispersion and size distributions of the inorganic fillers on the membranes. The inorganic particle samples for the TEM tests were prepared by ultrasonication of the powdered samples in ethanol and evaporation of one drop of the suspension onto a carbon film supported on a mesh copper grid. Nanocomposite samples for the TEM tests were prepared using a Leica Ultracut UCT microtome (Leica Microsystems GmbH, Germany). Thin sections of about 100 nm thickness were cut with a glass knife at room temperature at a rate of 1 mm/s. The cut sections, floating on the water in the boat, were collected with 300-mesh copper TEM grids. TEM was carried out at an accelerating voltage of 200 kV at room temperature.

The density of the sample was measured using an ultrapycnometer (Quantachrome Instruments, USA). Helium was used as the probe gas. For each test, the number of runs was set at 10, and the working cell size was medium.

A differential scanning calorimetry (DSC; 7 Sub-Amb, Perkin Elmer) was used to determine the glass transition temperature (T_g) of the membranes. These calorimetry tests were conducted under a temperature ramp from −20 to 400°C at a heating rate of 20°C/min. Taking the points of intersection as the onset and endpoint of the transition in the DSC curve, the T_g was located at one half the change in heat capacity between the onset and endpoint.

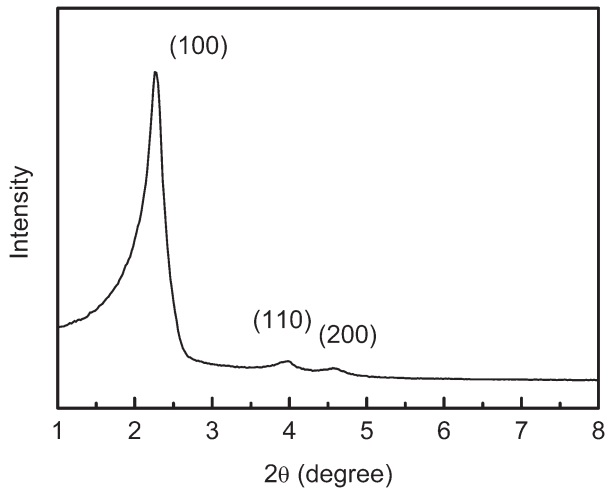

Figure 1. XRD pattern of synthesized MCM-41.

Single gas permeation tests of the pristine P84 membrane and the composite membranes were conducted using a constant volume and varying pressure experimental setup as described by Lua and Su.[28] A feed pressure of 4 bars was used for all the tests. Before the tests, the air in the whole system was completely evacuated using a pump (Adixen Drytel 1025) until the pressure of the downstream tank was down to 10^{-6} Torr. The single gases used in these tests were He, N_2, O_2, and CO_2. The purity of each gas was 99.99%. All the permeation tests were carried out under room temperature. The gas permeability (P) was determined as reported by Cong et al.,[29] and the unit is in Barrer [1 Barrer = 1×10^{-10} cm^3 (STP) cm/(cm^2 s cm Hg)]. The thickness of all the membranes was measured by a micrometer.

RESULTS AND DISCUSSION

Inorganic Filler Properties

The small-angle XRD pattern of the synthesized MCM-41 is shown in Figure 1. Three peaks in the $2\theta = 2°–6°$ range are clearly shown in the XRD pattern, and these peaks are associated to their corresponding *hkl* reflection indices, which are the characteristics of mesoporous MCM-41 material.[30] The N_2 adsorption–desorption isotherms of MCM-41 and nano-SiO_2 are shown in Figure 2. The curve for MCM-41 is a typical Type IV adsorption isotherm that indicates the characteristics of a mixed micro- and mesoporous material. The synthesized MCM-41 had a high-surface area of 812 m^2/g and a total pore volume of 0.67 cm^3/g as shown in Table I. According to the BJH method, the average pore size was about 2.7 nm. The curve for nano-SiO_2 is a typical Type II adsorption isotherm for nonporous materials. The BET surface area of nano-SiO_2 was 394 m^2/g as shown in Table I. The wide-angle XRD patterns of zeolite 4A, nano-SiO_2, and MCM-41 are shown in Figure 3. The XRD pattern of zeolite 4A showed many sharp peaks, indicating its good crystallinity, whilst the XRD patterns of nano-SiO_2 and MCM-41 exhibited only one broad peak each centred at 22.6°, indicating their amorphous structures. The TEM micrograph of MCM-41 particles in Figure 4 showed that they had a very narrow size distribution of 40–70 nm, which were obtained through a long period of hydrothermal aging during the synthesis procedure. The properties of all the three fillers are given in Table I, and their respective TEM micrographs are shown in Figure 4.

Table I. Properties of the Inorganic Fillers

Filler sample	Particle size (nm)	Pore size (nm)	Surface area (m^2/g)	Pore volume (cm^3/g)	Density (g/cm^3)
Fumed-silica	7	NA	394	NA	2.17
MCM-41	56	2.7	812	0.67	2.12
Zeolite 4A	2500	0.38	567	0.21	1.91

Membrane Morphology

The thickness of the pure P84 membrane was 32 μm, whilst the thicknesses of all the composite membranes were almost the

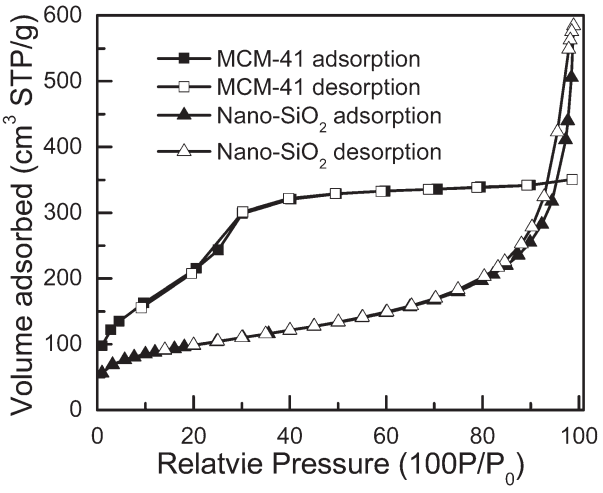

Figure 2. N_2 adsorption–desorption curves of synthesized MCM-41 and nano-SiO_2.

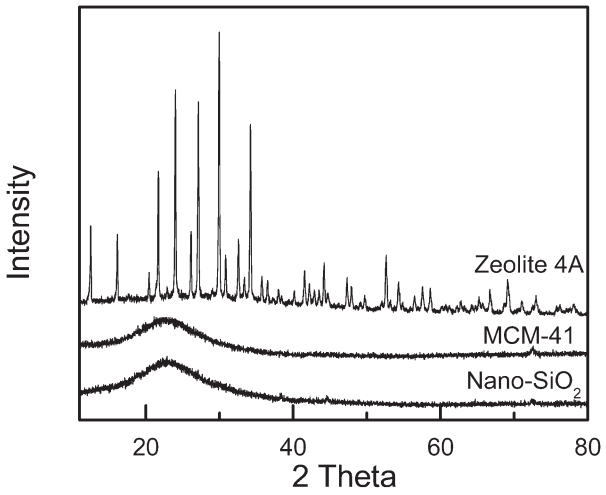

Figure 3. Wide-angle X-ray diffractions of zeolite 4A, MCM-41, and nano-SiO_2.

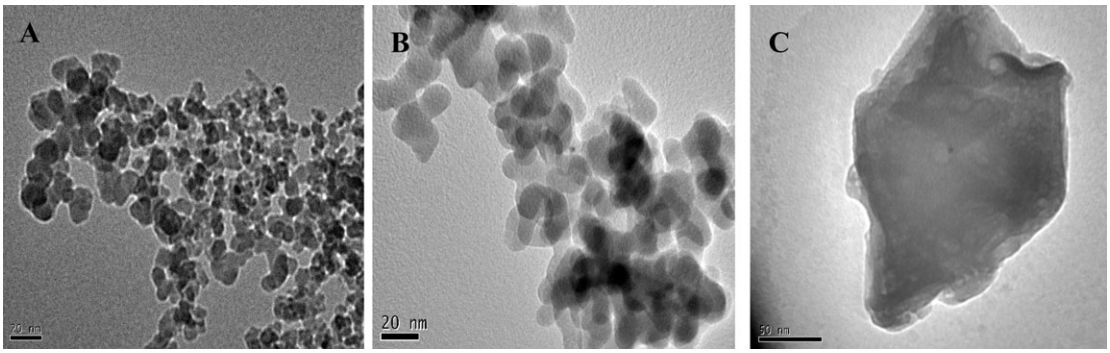

Figure 4. TEM micrographs of fumed nano-SiO_2 (A), synthesized MCM-41 (B), and zeolite 4A (C).

same, that is, 28 ± 1 μm, with slight thickness differences due to minor viscosity variations in the casting solutions. P84, P84/SiO_2, and P84/MCM-41 membranes were transparent, whilst the P84/4A membrane was slightly cloudy yellow and semitransparent in appearance.

Figure 5 shows the SEM micrographs of the P84 membrane and composite membranes, which are impregnated with filler particles that are well dispersed in the polymer matrix. The surface of the pure P84 membrane was very flat, as shown in Figure 5(1A). Based on the SEM micrographs of the top surfaces (2A, 3A), nano-SiO_2 and MCM-41 particles were well subembedded under the P84 surface. For the P84/4A composite membrane (4A), some zeolite 4A particles were partially exposed on the surface of the membrane because of their larger particle size (2500 nm, Table I) when compared with nano-SiO_2 (7 nm) and MCM-41 (56 nm) particles. Careful inspections revealed that some cavities existed in the cross-sections of P84/MCM-41 and P84/4A membranes, which were formed by the cleaving of MCM-41 and zeolite 4A particles from the polymeric matrix during the liquid nitrogen procedure, which was used to fracture the membranes during sample preparation for SEM analyses. In contrast, no such cavities were present in the membrane cross-sections of pure P84 (1B) and P84/SiO_2 (2B) membranes. From these micrographs, it could be seen that all the filler particles were well dispersed in the composite membranes although some silica particle aggregates of tens of nanometers were present. These clusters of silica particles are deemed as aggregates, because their pristine particle size is 7 nm as given in Table I. However, by mere observation of the SEM micrographs, it was not sufficiently convincing to draw conclusions that these filler particles had good wettability with the polymer chains and that no nonselective voids between the particle–polymer interfaces existed. Hence, to further investigate the wettability of the fillers and the nonexistence of voids in the composite membranes, TEM tests were carried out. TEM micrographs of the composite membranes are shown in Figure 6. The dark contrast in the micrographs corresponds to the inorganic particles, while the white contrast corresponds to the polymer chains. Figure 6 shows that the filler particles are well dispersed into the polymer matrix. It also confirmed that the inorganic particles had good compatibility with the polymer chains and that no voids were present between the particle–polymer interfaces.

Helium permeation through the membranes was also investigated as a function of its feed pressure. Figure 7 shows that for pure P84 membrane, He permeation is independent of the feed pressure. This behavior is characteristic of the permeation of nonplasticizing gases through glassy polymers. Similarly, He permeation through the P84/SiO_2 membrane is also independent of the feed pressure, whilst those of P84/MCM-41 and P84/4A membranes show slight increases with increasing feed pressure. Generally, for increasing feed pressure, a sharp increase in permeation will take place when some continuous nonselective voids or defects are present in the membranes. In this study, due to the low content of the fillers and with careful preparation, the filler particles were well dispersed in the membranes (Figure 5). The slight increases in the He permeation through P84/MCM-41 and P84/4A membranes with increasing feed pressure were not due to the presence of continuous voids between the particle–polymer interfacial areas. The pore sizes of MCM-41 and zeolite 4A particles were 2.7 and 0.38 nm, respectively. The transport of He molecules with a kinetic diameter of 0.26 nm through these nonselective pores of MCM-41 and zeolite 4A particles was dependent on the feed pressure, resulting in a slight increase of He permeability for the P84/MCM-41 and P84/4A composite membranes with increasing feed pressure.

Fractional Free Volume and DSC Results

The density of the composite membranes ρ was measured by an ultrapycnometer and was also calculated using eq. (1)

$$\rho = \frac{1}{\frac{1-w_f}{\rho_p} + \frac{w_f}{\rho_f}} \quad (1)$$

where ρ_p is the density of the P84 polymer powder, ρ_f is the density of the inorganic filler, and w_f is the weight fraction of the inorganic filler, which is 0.08 (8%) for all the three composite membranes in these tests. The properties of the inorganic fillers are given in Table I. The calculated density (ρ_c) and measured density (ρ_t) of the membranes are compared in Table II. The ρ_c values are slightly greater than the ρ_t values for the composite membranes; differences are as follows: P84/SiO_2—7.47%, P84/MCM-41—13.67%, and P84/4A—7.10%.

To understand the influence of the inorganic fillers on the polymer chain packing, the fractional free volume (FFV) of the pure

Applied Polymer SCIENCE

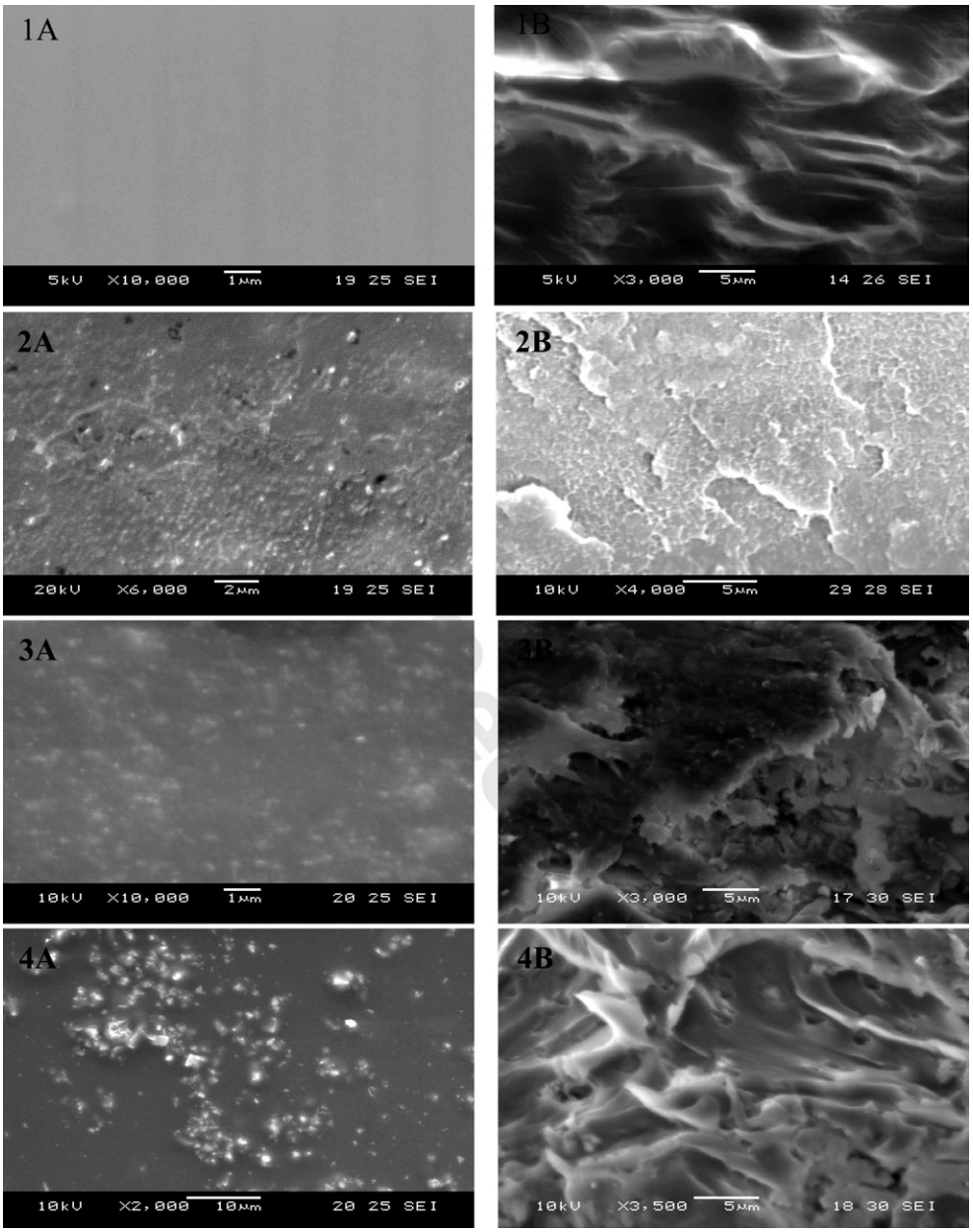

Figure 5. SEM micrographs of surface (A) and the cross-section (B) for P84 membrane (1), P84/8%SiO_2 membrane (2), P84/8%MCM-41 membrane (3), and P84/8%4A membrane (4).

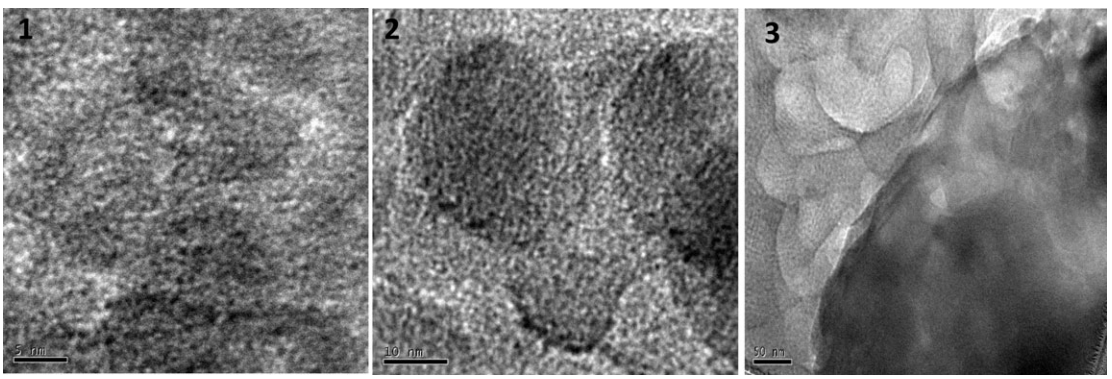

Figure 6. TEM micrographs of cut sections of (1) P84/SiO_2 membrane, (2) P84/MCM-41 membrane, and (3) P84/4A membrane.

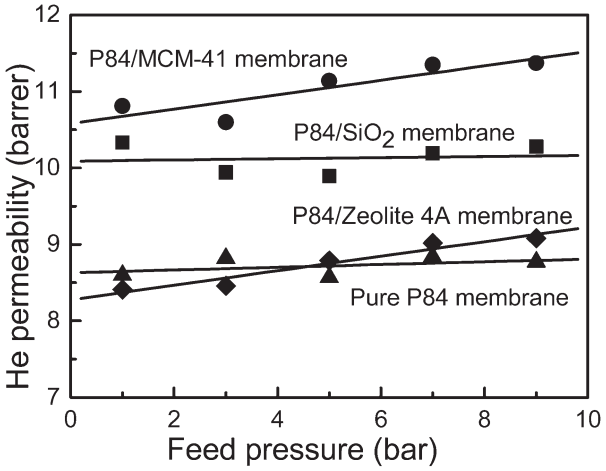

Figure 7. Dependence of He permeability on the feed pressure.

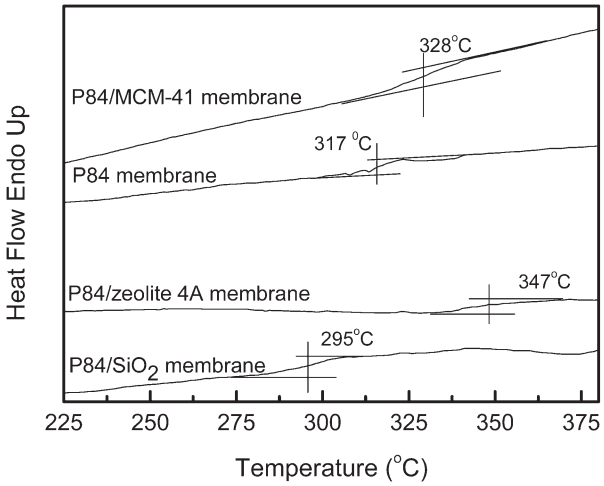

Figure 8. DSC curves of P84 membrane and composite membranes and their corresponding glass transition temperatures.

P84 membrane was estimated using eqs. (2), (2a), and (2b) as follows[31]:

$$\mathrm{FFV} = \frac{V - V0}{V} \tag{2}$$

$$V = M/\rho \tag{2a}$$

$$V0 = 1.3\ Vw \tag{2b}$$

where V is the total molar volume of P84 monomer (cm^3/mol), M is the molar mass of P84 monomer which is 423.6 g/mol, ρ is the density of the membrane, V_0 is the volume occupied by the polymer chains (cm^3/mol), and Vw is the van der Waals volume, which can be estimated by the group contribution method.[31] The value of Vw was found to be 194.5 cm^3/mol based on calculations according to Bos et al.[32]

For the composite membranes, the specific volume v (cm^3/g) can be obtained from the density tests. The volume occupied by the polymer chains as well as the inorganic fillers should be considered. The FFVs of the composite membranes were calculated using eqs. (3) and (3a) as follows:

$$\mathrm{FFV} = \frac{v - \left[v_0\left(1 - \varphi_f\right) + \varphi_f/\rho_f\right]}{v} \tag{3}$$

$$\varphi_f = \frac{w_f}{w_f + \frac{\rho_f}{\rho_p}(1 - w_f)} \tag{3a}$$

where φ_f is the volume fraction of the inorganic fillers and v_0 (cm^3/g) is the specific volume of the polymer chains. The calculated FFV values of the membranes are shown in Table II.

The DSC curves of pure P84 powder, P84 membrane, and composite membranes and their corresponding glass transition temperature (T_g) are shown in Figure 8. The T_g values of P84 powder and P84 membrane are 315 and 317°C, respectively, which agree with those of Bos et al.[33] The T_g value of the P84/SiO_2 membrane is 295°C, which is 22°C lower than that of the P84 membrane. In contrast to the P84/SiO_2 membrane, the T_g values of the P84/MCM-41 and P84/4A membranes are 328 and 347°C, respectively. Both are much higher than that of the P84 membrane.

Using molecular dynamic simulations for both experimental and modeling results, studies[34–37] have shown that the T_gs of composite materials could be enhanced or depressed depending on the properties of the polymer–particle interfaces. It is widely accepted that a free surface will have an effect on T_g. Some nanogaps or nonwetting interfaces between filler particles and polymer chains would decrease T_g, whereas an attractive polymer–particle interfacial interaction might increase T_g. For the P84/MCM-41 and P84/4A membranes, increases of 11 and 30°C, respectively, in the T_g over that of the P84 membrane were obtained as shown in Figure 8. This could be attributed to the immobilization of the polymer chains within the filler particle–polymer interaction areas by raising the energy barrier for the intermolecular chain movements. This phenomenon indicates that the MCM-41 and the zeolite 4A particles have good wettability to the polymer chains, supporting the thesis that the

Table II. Densities and Calculated Fractional Free Volumes of Membranes

Sample code	ρ_t (g/cm^3)	ρ_c (g/cm^3)	v (cm^3/g)	φ_f	FFV
P84 membrane	1.356	NA	0.737	0	0.190
P84/SiO_2	1.285	1.381	0.778	0.0509	0.242
P84/MCM-41	1.214	1.380	0.824	0.0521	0.284
P84/4A	1.281	1.372	0.781	0.0575	0.241

Table III. Single Gas Permeability and Ideal Selectivity of Gas Pairs

Sample code	PHe	PO_2	PN_2[a]	PCO_2	$\alpha He/O_2$	$\alpha O_2/N_2$	$\alpha CO_2/N_2$
Pure P84	8.60	0.41	0.049 ± 0.012	0.87	21.0	8.4	17.8
P84/SiO_2	10.33	0.59	0.078 ± 0.008	1.26	17.5	7.6	16.2
P84/MCM-41	10.81	0.67	0.181 ± 0.005	1.90	16.1	3.7	10.5
P84/Zeolite 4A	8.41	0.38	0.051 ± 0.014	0.81	22.1	7.4	15.9

[a]*Note:* As the N_2 permeation was very slow, three tests for each sample were carried out, and the average permeability was obtained. The unit for the permeability is Barrer.

slight increases in He permeations through the P84/MCM-41 and P84/4A membranes in Figure 6 do not result from the nonselective voids. In contrast to the P84/MCM-41 and P84/4A membranes, the P84/SiO_2 membrane showed a decrease in T_g when compared with the P84 membrane. Generally, a decrease in *Tg* for nanocomposite membrane is attributed to the large particle/polymer interfacial area, which is similar to nanoscale thin films with large surface area to volume ratios.[37] In the P84/SiO_2 membrane, the size of SiO_2 was about 7 nm, which was much smaller than those of MCM-41 and zeolite 4A particles (Table I). This smaller SiO_2 size was much more effective in disrupting chain packing and increasing the distance between molecular chains. As a result, large numbers of particle–polymer interface areas existed in the P84/SiO_2 membrane, resulting in a decrease in T_g as shown in Figure 8.

The density of pure P84 powder was found to be 1.339 g/cm^3, which was very close to the reported value of 1.336 g/cm^3 by Bos et al.[33] For the composite membranes, the theoretical density estimated by eq. (1) was larger than the measured value, suggesting an increase in the free volume of the polymer with the introduction of filler particles.[9,10] This was also verified by the calculated fractional free volume values in Table II. The FFV of P84 membrane was calculated as 0.19, which was slightly smaller than the previously reported value of 0.20.[32] This difference could be due to the different casting solvent or thermal treatments. The FFV values of composite membranes were larger than that of P84 membrane. This could be explained by the fact that the filler particles changed the chain structure and decreased the chain packing density by disordering the molecular chains. From Table II, the P84/SiO_2 membrane had a smaller FFV value than that of P84/MCM-41 membrane. The fumed SiO_2 particles, with much smaller sizes, should be more effective in disrupting chain packing, and the P84/SiO_2 membrane should have a larger particle–polymer interface area and FFV value than those of the P84/MCM-41 and P84/4A membranes. However, the larger calculated FFV values of the P84/MCM-41 and P84/4A membranes might be attributed to the fact that MCM-41 and zeolite 4A particles were porous. A part of the pore volume of these particles, which was not part of the polymer chains, also contributed to the bulk-specific volume during the FFV analysis. If the particle voids were accounted for and making the assumption that no polymer chains were trapped into the pores of the MCM-41 and the zeolite 4A particles, new FFV values of 0.24 and 0.22 should be used for the P84/MCM-41 and the P84/4A membranes, respectively, after subtracting the pore volume of the filler particles from the bulk-specific volume.

Gas Permeation Results

Generally, the physical characteristics of the membranes such as the particle–polymer interfaces, the FFV values, and the properties of the filler particles are consistent with the transport behaviors of the composite membranes as shown in the gas permeation results in Table III. Table III shows the permeability and selectivity results for the various gases (He, O_2, N_2, and CO_2) for the P84 membrane and composite membranes. The ideal selectivity (α) of a membrane for gas pair (A/B) is defined as the ratio of the permeability (P) of gas A to that of gas B. For the tests carried out here, the P84 membrane showed slightly lower permeabilities for He, CO_2, O_2, and N_2 when compared with the previously reported values.[33] The lower permeability could be due to the long heat treatment time during the membrane preparation. In Table III, the P84/MCM-41 composite membrane yielded the highest permeability value for all the single gases. The permeabilities of He, O_2, N_2, and CO_2 were 10.81, 0.67, 0.181, and 1.9 Barrer, respectively. However, the selectivities of gas pairs (He/O_2, O_2/N_2, and CO_2/N_2) for the P84/MCM-41 composite membrane were the lowest amongst all the membranes tested. For example, α of O_2/N_2 and α of CO_2/N_2 resulted in percent reductions of 56% and 41%, respectively, when compared with those of P84 membrane. Some composite membranes yield high-gas permeation but suffer low selectivity due to the presence of nonselective voids in the membranes. However, the MCM-41 composite membrane in this study had been shown to be free of these nonselective voids as verified by the TEM micrograph in Figure 6. In this case, the probable reasons could be twofold. First, the MCM-41 particles with sizes of about 56 nm could disrupt the chain packing and increase the free volume of the polymer chain. Second, the transport of molecules through the channels of MCM-41 (2.7 nm) was much faster than through the P84 polymer chains. These channels were much larger and nonselective for all the test gases. As a result of these combined effects, a lower selectivity for the P84/MCM-41 composite membrane was observed when compared with the other composite membranes and the P84 membrane.

In contrast to the P84/MCM-41 composite membrane, the P84/4A composite membrane showed slightly lower permeabilities for He, O_2, and CO_2, and comparable permeability for N_2 when compared with the P84 membrane. However, the selectivities of the gas pairs, except for He/O_2, showed no improvements over those of P84 membrane. Generally, the introduction of zeolite 4A particles into the polymer matrix membranes was believed to enhance the selectivity of gas separation due to their

molecular sieving pore size of 0.38 nm. In this study, the reductions in both the gas permeability and selectivity for P84/4A composite membrane could be due to the rigidifications of the polymer chains around the surfaces and pores of the zeolite 4A particle, resulting in the increase of the tortuosity of the transport path of gas molecules. This phenomenon was also reported by Moore and Koros.[20,21] The rigidifications of the polymer chains could be due to the long thermal treatment time, and this deduction is supported by the significant increase of 30°C in the T_g of the P84/4A composite membrane over that of the P84 membrane.

In Table III, the permeabilities of He, O_2, N_2, and CO_2 for the P84/SiO_2 membrane are 10.33, 0.59, 0.078, and 1.26 Barrer, respectively, corresponding to increases of 20, 63, 59, and 45%, respectively, in the permeabilities over those of the P84 membrane. Correspondingly, the selectivities of gas pairs (α He/O_2, α O_2/N_2, and α CO_2/N_2) for the P84/SiO_2 membrane showed slight decreases to those of the P84 membrane. Merkel et al.[9,10] attributed the high permeation of fumed nano-SiO_2 composite membranes to their large free volumes. They suggested that nano-SiO_2 particles could disrupt the rigid polymer chain packing and lead to a large free volume of polymer chains. The larger free volume enabled the chains to have more space and lower energy barriers to move. It is accepted that the flexible movements of the polymer chains are favorable to the transport of gas molecules. In comparison with the mesoporous MCM-41 particles of size 56 nm and the microporous zeolite 4A particles of size 2500 nm as shown in Table I, the nano-SiO_2 particles had the smallest particles size of 7 nm and could most effectively disorder the glassy P84 chains and create a large free volume in the P84/SiO_2 membrane as indicated by the FFV calculations (Table II). Therefore, the P84/SiO_2 membrane has a high permeability whilst maintaining good selectivity. The nano-SiO_2 particles were nonporous and therefore impervious to the transport of gas molecules within the particles, having no effects on the permeability and selectivity of the membrane. Similar to the P84/MCM-41 composite membrane, the P84/SiO_2 composite membrane had also been shown to be free of nonselective voids at the inorganic filler particle–polymer interface as verified by the TEM micrograph in Figure 6 and therefore would not affect the transport of gas molecules at these interface areas. The gas-separation performances of the resulting membranes were compared to the well-known Robeson's upper bound. The CO_2/N_2 selectivities/permeabilities of the four membranes were found to be below the Robeson's upper bound. The P84/SiO_2 membrane was slightly better than the pure P84 membrane with reference to the Robeson's upper bound as shown in Figure 9. Among the four membranes, the P84/SiO_2 membrane provided the best separation performance.

CONCLUSIONS

Three types of inorganic fillers—fumed nano-SiO_2, synthesized mesoporous MCM-41, and zeolite 4A—were incorporated into the P84 polymer matrix to prepare mixed matrix membranes. The influences of the presence of these fillers on the structure of the polymer chains and the gas transport properties had been investigated.

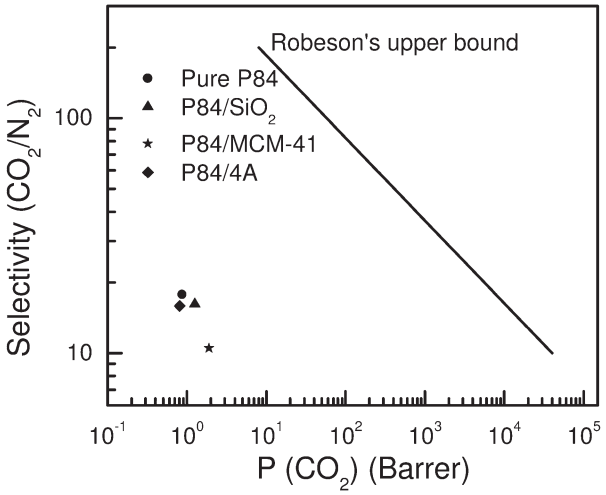

Figure 9. Comparison of the separation of CO_2/N_2 with Robeson's upper bound.

The SEM micrographs indicated that the filler particles were well dispersed in the polymer matrix, whilst the TEM micrographs verified that there were no voids at the particle–polymer interfaces. Increases in the glass transition temperature (T_g) of 11 and 30°C were observed for the P84/MCM-41 and P84/4A membranes, respectively, which were above that of the P84 membrane, whilst a 22°C decrease was observed for the P84/SiO_2 membrane when compared with that of the P84 membrane. Density tests and FFV calculations revealed that the introduction of the fillers, especially the fumed nano-SiO_2 particles, changed the polymer chain structure and effectively increased the free volume of the polymer chains.

Gas permeation tests for He, O_2, N_2, and CO_2 were carried out on the pure P84 membrane as well as the composite membranes. It was found that gas permeation was dependent on the type of filler particles and their physical characteristics (such as particle size and pore size) and the properties of the particle–polymer interface. The P84/4A composite membrane showed slight decreases in the permeability and selectivity when compared with those of the P84 membrane because of the rigidification of the polymer chains around the surfaces of the zeolite particles. P84/MCM-41 membrane showed the highest permeability but the lowest gas selectivity due to the faster transport of molecules through the channels of MCM-41 particles with average pore size of 2.7 nm. P84/SiO_2 membrane had better gas separation performance with higher permeability and acceptable gas selectivity than the other membranes. In comparison with the P84 membrane, the P84/SiO_2 membrane showed increases of 20, 63, 59, and 45% in permeabilities for He, O_2, N_2, and CO_2, respectively.

REFERENCES

1. Alexander, S. S. *J. Membr. Sci.* **1994**, *94*, 1.
2. Koros W. J.; Fleming, G. K. *J. Membr. Sci.* **1993**, *83*, 1.
3. Chung, T. S.; Jiang, L. Y.; Li, Y.; Kulprathipanja, S. *Prog. Polym. Sci.* **2007**, *32*, 483.

4. Robeson, L. M. *J. Membr. Sci.* **1991**, *62*, 165.
5. Boom, J. P.; Punt, I.; Zwijnenberg, H.; de Boer, R.; Bargeman, D.; Smolders, C. A.; Strathmann, H. *J. Membr. Sci.* **1998**, *138*, 237.
6. Pechar, T. W.; Kim, S.; Vaughan, B.; Marand, E.; Tsapatsis, M.; Jeong, H. K.; Cornelius, C. J. *J. Membr. Sci.* **2006**, *277*, 195.
7. Mahajan, R.; Koros, W. *J. Ind. Eng. Chem. Res.* **2000**, *39*, 2692.
8. Wang, H. T.; Holmberg, B. A.; Yan, Y. S. *J. Mater. Chem.* **2002**, *12*, 3640.
9. Merkel, T. C.; Freeman, B. D.; Spontak, R. J.; He, Z.; Pinnau, I.; Meakin, P.; Hill, A. *J. Science* **2002**, *296*, 519.
10. Merkel, T. C.; Freeman, B. D.; Spontak, R. J.; He, Z.; Pinnau, I.; Meakin, P.; Hill, A. *J. Chem. Mater.* **2003**, *15*, 109.
11. Kim, S.; Marand, E.; Ida, J.; Guliants, V. V. *Chem. Mater.* **2006**, *18*, 1149.
12. Reid, B. D.; Ruiz-Trevino, F. A.; Musselman, I. H.; Balkus, K. J.; Ferraris, J. P. *Chem. Mater.* **2001**, *13*, 2366.
13. Jeong, H. K.; Krych, W.; Ramanan, H.; Nair, S.; Marand, E.; Tsapatsis, M. *Chem. Mater.* **2004**, *16*, 3838.
14. Cong, H. L.; Zhang, J. M.; Maciej, R.; Shen, Y. Q. *J. Membr. Sci.* **2007**, *294*, 178.
15. Gomes, D.; Nunes, S. P.; Peinemann, K. V. *J. Membr. Sci.* **2005**, *24*, 613.
16. Li, Y.; Chung, T. S.; Cao, C.; Kulprathipanja, S. *J. Membr. Sci.* **2005**, *260*, 45.
17. Sullivan, D. M.; Bruening, M. L. *Chem. Mater.* **2003**, *15*, 281.
18. Joly, C.; Smaihi, M.; Porcar, L.; Noble, R. D. *Chem. Mater.* **1999**, *11*, 2331.
19. Zhong, S. H.; Li, C. F.; Xiao, X. F. *J. Membr. Sci.* **2002**, *199*, 53.
20. Moore, T. T.; Koros, W. J. *J. Membr. Sci.* **2005**, *73*, 987.
21. Mahajan, R.; Buins, R.; Schaeffer, M.; Koros, W. J. *J. Appl. Polym. Sci.* **2002**, *86*, 881.
22. Mahajan, R.; Koros, W. *J. Polym. Eng. Sci.* **2002**, *42* 1420.
23. Garcia, M. G.; Marchese, J.; Ochoa, N. A. *J. Appl. Polym. Sci.* **2010**, *118*, 2417.
24. Kumar, S.; Rath, T.; Mahaling, R. N.; Reddy, C. S.; Das, C. K.; Pandey, K. N.; Srivastava, R. B.; Yadaw, S. B. *Mater. Sci. Eng. B* **2007**, *141*, 61.
25. Vu, D. Q.; Koros, W. J.; Miller, S. J. *J. Membr. Sci.* **2003**, *211*, 311.
26. Grun, M.; Unger, K.; Matsumoto, A.; Tsutsumi, K. *Microporous Mesoporous Mater.* **1999**, *27*, 207.
27. Qiao, X. Y.; Chung, T. S.; Rajagopalan, R. *Chem. Eng. Sci.* **2006**, *61*, 6816.
28. Lua, A. C.; Su, J. C. *Carbon* **2006**, *44*, 2964.
29. Cong, H. L.; Hu, X. D.; Radosz, M.; Shen, Y. Q. *Ind. Eng. Chem. Res.* **2007**, *46*, 2567.
30. Beck, J. S.; Vartuli, J. C.; Roth, W. J.; Leonowicz, M. E.; Kresge, C. T.; Schmitt, K. D.; Chu, C. T.-W.; Olson, D. H.; Sheppard, E. W.; McCullen, S. B.; Higgins, J. B.; Schlenkert, J. L. *J. Am. Chem. Soc.* **1992**, *114*, 10835.
31. Park, J. Y.; Paul, D. R. *J. Membr. Sci.* **1997**, *125*, 23.
32. Bos, A.; Punt, I.; Wessling, M. *J. Membr. Sci.* **1999**, *155*, 67.
33. Bos, A.; Punt, I.; Strathmann, H.; Wessling, M. *AIChE J.* **2001**, *47*, 1088.
34. Brown, D.; Marcadon, V.; Mele, P.; Alberola, N. D. *Macromolecules* **2008**, *41*, 1499.
35. Rittigstein, P.; Priestley, R. D.; Broadbelt, L. J.; Torkelson, J. M. *Nat. Mater.* **2007**, *6*, 278.
36. Bansal, A.; Yang, H. C.; Li, C. Z.; Cho, K. W.; Benicewicz, B. C.; Kumar, S. K.; Schadler, L. S. *Nat. Mater.* **2005**, *4*, 693.
37. Ash, B. J.; Siegel, R. W.; Schadler, L. S. *J. Polym. Sci., Part B: Polym. Phys.* **2004**, *42*, 4371.